



Cite this: *Phys. Chem. Chem. Phys.*,
2016, **18**, 16555

Understanding M–ligand bonding and *mer-/fac-*isomerism in tris(8-hydroxyquinolate) metallic complexes†

Carlos F. R. A. C. Lima,^{*ab} Ricardo J. S. Taveira,^a José C. S. Costa,^{ac}
Ana M. Fernandes,^b André Melo,^d Artur M. S. Silva^b and Luís M. N. B. F. Santos^{*a}

Tris(8-hydroxyquinolate) metallic complexes, Mq_3 , are one of the most important classes of organic semiconductor materials. Herein, the nature of the chemical bond in Mq_3 complexes and its implications on their molecular properties were investigated by a combined experimental and computational approach. Various Mq_3 complexes, resulting from the alteration of the metal and substitution of the 8-hydroxyquinoline ligand in different positions, were prepared. The *mer-/fac-*isomerism in Mq_3 was explored by FTIR and NMR spectroscopy, evidencing that, irrespective of the substituent, *mer-* and *fac-*are the most stable molecular configurations of Al(III) and In(III) complexes, respectively. The relative M–ligand bond dissociation energies were evaluated experimentally by electrospray ionization tandem mass spectrometry (ESI-MS-MS), showing a non-monotonous variation along the group (Al > In > Ga). The results reveal a strong covalent character in M–ligand bonding, which allows for through-ligand electron delocalization, and explain the preferred molecular structures of Mq_3 complexes as resulting from the interplay between bonding and steric factors. The *mer*-isomer reduces intraligand repulsions, being preferred for smaller metals, while the *fac*-isomer is favoured for larger metals where stronger covalent M–ligand bonds can be formed due to more extensive through-ligand conjugation mediated by metal “d” orbitals.

Received 19th April 2016,
Accepted 31st May 2016

DOI: 10.1039/c6cp02608g

www.rsc.org/pccp

Introduction

Metallic complexes based on 8-hydroxyquinoline belong to one of the most important classes of electroluminescent and electron transport materials largely used as constituents of organic light emitting diodes (OLEDs).¹ Generally abbreviated as Mq_3 , these compounds are coordination complexes wherein the trivalent metal, M(III), is bonded to three bidentate 8-hydroxyquinolate ligands (q). Among the Mq_3 , tris(8-hydroxyquinolate)-aluminium(III), Alq_3 , was the first to be used in OLEDs, since the pioneering work of Tang and Van Slyke.² This compound is extensively used in organic electronics because of its thermal stability; ease of synthesis, purification, and physical-vapour

deposition; and exceptional electron transport and electroluminescent properties as an organic thin film.³ According to the literature, Gaq_3 and Inq_3 , and more recently some substituted Mq_3 complexes, can also present notable electronic properties and electroluminescence yields, which makes them promising alternatives as emitting and charge transport materials.⁴ Moreover, the introduction of small substituents in the ligands or subtle structural changes in Mq_3 complexes offer, not only a simple way to explore tunable materials, but also a powerful systematic approach to study the molecular, optical and charge transport properties of these compounds at a more fundamental level.

Metallic Mq_3 complexes have octahedral geometry and can occur in two different stereoisomers: meridional (*mer-*) and facial (*fac-*), as depicted in Fig. 1.

The efficiency, stability and emission behaviour of organic electronic devices based on Mq_3 complexes are influenced by their molecular configuration (e.g. *mer*- Alq_3 has green and *fac*- Alq_3 has blue light emission).⁵ In OLEDs, *fac*-isomers are particularly desirable due to their blue-shifted fluorescence and high quantum yield.⁵ The *mer*-isomers of Alq_3 and Gaq_3 are observed at ambient conditions and can be converted to the *fac*-isomers by annealing at $T > 650$ K.⁶ For Alq_3 various

^a CIQ, Departamento de Química e Bioquímica, Faculdade de Ciências da Universidade do Porto, Porto, Portugal. E-mail: carlos.chemistry@gmail.com, lbsantos@fc.up.pt

^b Department of Chemistry & QOPNA, University of Aveiro, Aveiro, Portugal

^c LEPABE, Faculdade de Engenharia da Universidade do Porto, Porto, Portugal

^d LAQV-REQUIMTE, Departamento de Química e Bioquímica, Faculdade de Ciências da Universidade do Porto, Porto, Portugal

† Electronic supplementary information (ESI) available: Detailed synthesis data and compound characterization; detailed FTIR, UV-Vis, NMR, mass spectrometry and computational results. See DOI: 10.1039/c6cp02608g

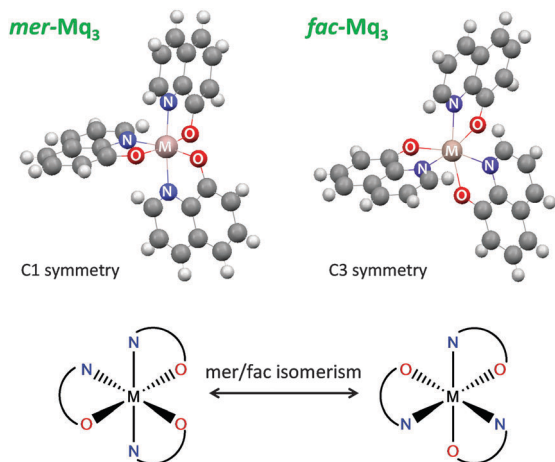


Fig. 1 Schematic representation of the *mer*-/*fac*-isomerism in Mq_3 complexes.

polymorphic structures were observed and characterized by crystallography and spectroscopy.^{5d,e,7} The polymorphs have distinct morphological and electronic properties according to whether they contain the *mer*- or *fac*-isomers and to their crystal packing, thus affecting the performance of the organic devices into which they may be incorporated. Although the *mer*-isomer is likely the most stable molecular configuration of Alq_3 and Gaq_3 , the case of Inq_3 is more uncertain, with the *fac*-isomer appearing as the most stable at room temperature.^{6d,8} The tendency across the group gets more puzzling since Tlq_3 was found to be *mer*.⁹ Gas phase theoretical studies indicate that the *mer*-isomer is energetically more stable by $\approx 20 \text{ kJ mol}^{-1}$ in all Mq_3 complexes ($M = Al(III), Ga(III), In(III)$).^{6d,10} This difference is high enough to guarantee that under most conditions the *fac*-isomers would not be experimentally observable, thus suggesting the inadequacy of the generally used theoretical methods for these studies. The knowledge about the nature of the chemical bond in Mq_3 complexes helps to understand their structural preferences and provides insights about their chemical stability, and charge transport and optical properties. However, the literature reports on this subject are still scarce and inconclusive.^{1a,11}

In the light of this state-of-the-art, a better understanding about the molecular stability of Mq_3 complexes is required. Herein, the effects of metal and ligand substitution on the molecular isomerism and M–ligand bond strength in Mq_3 were investigated experimentally and theoretically by spectroscopic, mass spectrometry and DFT studies for the compounds presented in Fig. 2.

This research aims to: (a) establish which factors most influence *mer*-/*fac*-isomerism; (b) define bonding patterns in Mq_3 complexes. The performance of organic electronic devices depends significantly on the molecular and supramolecular properties of their constituents. Therefore, the insights obtained in this work are of fundamental importance for understanding the exceptional properties of Mq_3 compounds as organic semiconductors, and to guide research in the quest for tunable and improved organic materials for a variety of sustainable energy technologies.

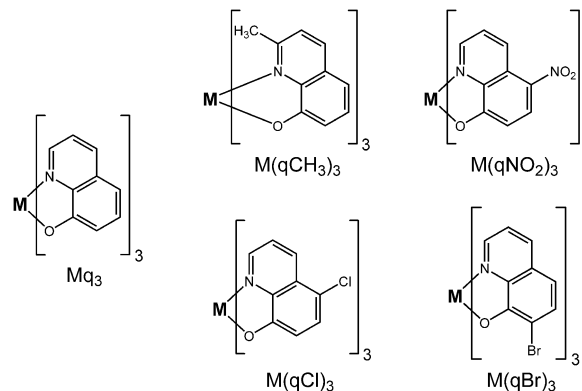


Fig. 2 Structural formulae of the Mq_3 complexes studied herein ($M = Al(III), In(III)$) and adopted acronyms.

Experimental

Synthesis and purification of the metallic complexes

All the metallic complexes under study (Fig. 2) were synthesized by reacting the metal chloride MCl_3 ($M = Al(III), In(III)$) with the corresponding 8-hydroxyquinoline ligand in a basic (KOH) solution of $H_2O/EtOH$. All starting reagents were obtained commercially and used without further purification.

General synthetic procedure. A solution of metal(III) chloride (1 mol equiv.⁻¹) and 8-hydroxyquinoline derivative (3.5 mol equiv.⁻¹) in 50 ml of $H_2O/EtOH$ (1 : 1) was maintained under stirring at $T = 60 \text{ }^\circ\text{C}$. After complete dissolution of the two reactants a solution of KOH (4 mol equiv.⁻¹) in 25 ml of H_2O was added and the mixture maintained at $60 \text{ }^\circ\text{C}$ under stirring for 2 hours. The yellow precipitate formed was filtered and washed with water, ethanol and acetone. The resulting solid was purified by heating under vacuum in order to remove residues of free 8-hydroxyquinoline ligand and other volatile impurities. The overall reaction yields were in the order of 50–80%. The purity of the samples was accessed by the spectroscopic studies used for compound characterization, showing the presence of minor (<2 mol%) impurities (*e.g.* free 8-hydroxyquinoline ligand) in all cases. The detailed synthesis and characterization data for all complexes studied are presented as the ESI.† The synthesis and purification of the unsubstituted metallic complexes of tris(8-hydroxyquinolate) of $Al(III), Alq_3, Ga(III), Gaq_3,$ and $In(III), Inq_3,$ were reported in a previous study.^{6d}

General spectroscopic techniques

The FTIR spectra of solid samples of the Mq_3 complexes studied and of the free ligands were recorded at $T = 298.1 \text{ K}$ using a FTIR Spectrum BX equipped with an ATR Pike Technologies GladiaATR™ sample holder. The UV-Vis spectra of all Mq_3 complexes and of the free ligands in CH_2Cl_2 , at $T = 298.1 \text{ K}$, were recorded with an Agilent 8453 diode array UV-Vis spectrometer, using a quartz cell with a path length of 10.00 mm. Temperature control was achieved by means of a Julabo F25 HP refrigerated circulator. The concentration of the samples was in the order of 10^{-5} M .

Solution and solid NMR spectroscopy

The 1D ^1H and ^{13}C , and 2D ^1H NOESY and ^{15}N HMBC NMR spectra in solution of the synthesized Mq_3 complexes and of the free ligands were recorded on a Bruker Avance 300 [operating at 300.13 MHz (^1H), 75.47 MHz (^{13}C)] spectrometer, at $T = 298$ K, using TMS as internal reference and CDCl_3 as the solvent. The solid state ^{13}C CP/MAS NMR spectra of the Mq_3 complexes and of the free ligands were acquired on a Bruker Avance 400 spectrometer.

Mass spectrometry studies

Electrospray ionization mass spectra (ESI-MS) and tandem mass spectra (ESI-MS-MS) were acquired with a Micromass Q-ToF 2 (Micromass, Manchester, UK), operating in the positive ion mode, equipped with a Z-spray source. Source and desolvation temperatures were 353 K and 373 K, respectively. The Mq_3 compounds were dissolved in CHCl_3 , the solutions thus obtained diluted in CH_3OH /trifluoroacetic acid (0.1%) and introduced at $10 \mu\text{l min}^{-1}$ flow rate into the electrospray ion source. The capillary and the cone voltage were 3000 V and 30 V, respectively. Nitrogen was used as nebulisation gas and argon as collision gas. ESI-MS-MS spectra were acquired by selecting the precursor ion with the quadrupole, performing collisions with argon at variable energies (E_{Lab}) in the hexapole and analysing the fragment ions thus produced with the TOF analyser. The spectra represent an average of approximately 100 scans. To implement energy-variable collision induced dissociation the applied collisional activation voltage (E_{Lab}) is increased by small increments while the relative abundances of the precursor and fragment ions are monitored. The energy required to dissociate 50% of the precursor ion was registered as $E_{\text{Lab},1/2}$. In this inelastic collision of the projectile ion with the target neutral, the total available energy for conversion of translational (or kinetic) to internal (or vibrational) energy of the projectile ion is the center of mass energy, E_{cm} , which can be calculated from $E_{\text{Lab},1/2}$ and the masses for the neutral target (m_t) and precursor ion (m_p), according to eqn (1):

$$E_{\text{cm}} = E_{\text{Lab}} \left(\frac{m_t}{m_p + m_t} \right) \quad (1)$$

Computational chemistry calculations

All quantum chemical calculations were performed using the Gaussian 09 software package.¹² The optimized geometries and respective electronic energies for Mq_3 and Mq_2 complexes and the free ligands were computed at the M06-2X/6-31+G(d,p)/SDD level of theory (the SDD Effective Core Potential basis set was used for the heavy atoms of Ga, In and Br, and 6-31+G(d,p) was used for the other atoms).¹³ Frequency calculations, at the M06-2X/6-31+G(d,p)/SDD level, were performed for both the *mer*- and *fac*-isomers of Alq_3 , Gaq_3 and Inq_3 , and for some other relevant molecular species – no imaginary frequencies were found, confirming that the structures correspond to true minima. The corresponding electronic energies were corrected for the zero-point energy (ZPE) and thermal enthalpies to $T = 298.15$ K,

using no scaling factors (this is a reasonable approximation for relative comparisons of molecular energetics). NBO point charges were calculated for all 8-hydroxyquinolinate ligands at the M06-2X/6-31+G(d,p)/SDD level of theory. The use of the M06-2X functional ensures that dispersive interactions, which are important for describing intraligand interactions in the complexes, are taken into account.¹³ All calculations were performed without symmetry restrictions.

Results and discussion

General remarks

The characterization data of all studied Mq_3 complexes confirms the expected structures and are consistent with a hexacoordinated octahedral geometry.

Evaluation of *mer*-/*fac*-isomerism

Fig. 3 shows the different protons in the 8-hydroxyquinolinate structure. The ^1H (presented in Fig. 4) and ^{13}C (presented as the ESI $^+$) NMR spectra in solution show a clear distinction between the Al(III) and In(III) complexes.

The Al(III) species present more complex spectra, with more peaks and less equivalent protons, while the spectra of In(III) complexes are simpler and better resolved. This indicates that in CDCl_3 solution, irrespective of the substituent, the Al(III) complexes adopt the *mer*-configuration (where all ligands are spatially different and chemically non-equivalent), while the more symmetric *fac*-isomer (where all ligands are equivalent) is the preferred one in In(III) complexes. The NMR spectra of $\text{Al}(\text{qCH}_3)_3$, for which decomplexation occurred in solution (the spectrum presented in Fig. 4 for this compound corresponds to the free ligand), and $\text{Al}(\text{qBr})_3$, which has very low solubility in CDCl_3 , could not be recorded. Although in the *mer*-isomer all three ligands are non-equivalent, only $\text{Al}(\text{qNO}_2)_3$ presents three sets of distinguishable resonance signals. In the other complexes of Al(III), Alq_3 and $\text{Al}(\text{qCl})_3$, only two sets of signals (in a 2 : 1 ratio) can be distinguished, with two ligands being chemically similar and producing superimposed peaks. It can also be noted that the change in the chemical shifts of 8-hydroxyquinoline upon complexation is more significant for the complexes with the $-\text{NO}_2$ group, $\text{Al}(\text{qNO}_2)_3$ and $\text{In}(\text{qNO}_2)_3$. This can be related with the strong electron withdrawing and polarizing capabilities of the $-\text{NO}_2$ group, and will be discussed in more detail later.

The *mer*-/*fac*-isomerism in the solid phase was evaluated by FTIR and solid state NMR spectroscopy. The comparison between

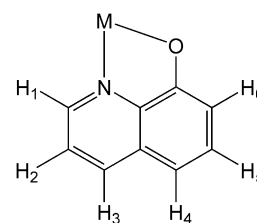


Fig. 3 Molecular structure of the 8-hydroxyquinolinate ligand showing the six different protons.

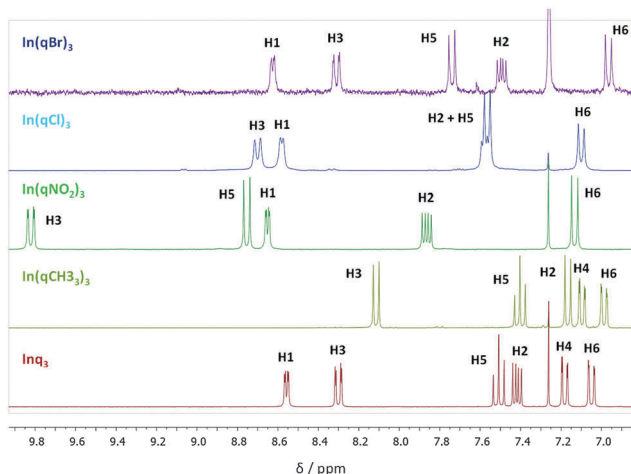
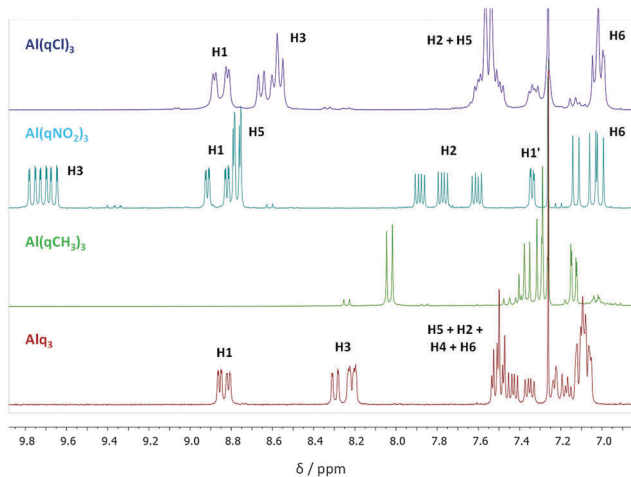


Fig. 4 ^1H NMR spectra, in CDCl_3 , of the Mq_3 complexes, $\text{M} = \text{Al(III)}$ (top), In(III) (bottom) in the aromatic region. Peak assignment is based on Fig. 3.

the FTIR spectra of the free 8-hydroxyquinolate ligands and the corresponding Al(III) or In(III) complexes clearly shows the disappearance of the broad $-\text{OH}$ peak of quinoline (at $\sim 3200\text{ cm}^{-1}$) and the appearance of two peaks at ~ 1100 and $\sim 1300\text{ cm}^{-1}$, which indicate formation of the $\text{M}-\text{O}$ bond. These results corroborate the successful synthesis of the complexes and their purity (no significant quantities of the free ligands were detected). Fig. 5 presents two regions of the FTIR spectrum where some differences between the complexes can be observed. In the fingerprint region ($800\text{--}400\text{ cm}^{-1}$) a systematic differentiation between the Al(III) and In(III) complexes is detected. The simulated FTIR spectra (unscaled frequencies at the M06-2X/6-31+G(d,p) level, presented as the ESI^\dagger) for isolated Alq_3 and Inq_3 indicate only minor differences between the *mer*- and *fac*-isomers in this region but are in agreement with the experimental results when comparing between the two metals. These results suggest that these spectral differences are mostly related with the identity of the central metal and have small dependence on the molecular configuration adopted by the complex. In the $1400\text{--}800\text{ cm}^{-1}$ region the differences between Al(III) and In(III) complexes are more subtle. While for the $\text{M(qNO}_2)_3$ and M(qBr)_3 cases the Al(III) and In(III) spectra are

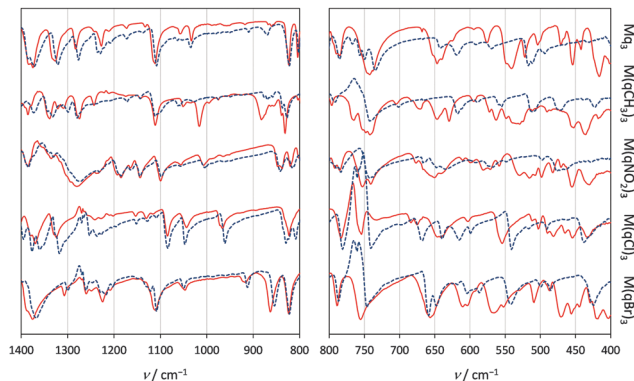


Fig. 5 FTIR spectra of the solid Mq_3 complexes studied ($\text{M} = \text{Al(III)}$, In(III)) in the selected regions (left: $1400\text{--}800\text{ cm}^{-1}$, right: $800\text{--}400\text{ cm}^{-1}$): $\text{M} = \text{Al(III)}$ (red solid lines); $\text{M} = \text{In(III)}$ (blue dotted lines).

virtually superimposed (high degree of peak matching), for Mq_3 , $\text{M(qCH}_3)_3$ and M(qCl)_3 there is a lower degree of similarity (e.g. in $\text{Al(qCH}_3)_3$ there is a strong peak at $\sim 1010\text{ cm}^{-1}$ that is absent in $\text{In(qCH}_3)_3$). Also considering that the $\text{C}-\text{O}$ bond stretching modes lie within this spectral window these differences might be related with *mer*-/*fac*-isomerism. The question of which *mer*- or *fac*-isomer is present in each compound cannot be answered accurately by FTIR. However, these results suggest that if configurational differences exist between Al(III) and In(III) complexes in the solid phase, they are more likely in Mq_3 , $\text{M(qCH}_3)_3$ and M(qCl)_3 .

Fig. 6 presents the ^{13}C CP/MAS NMR spectra of the solid Al(III) and In(III) complexes studied. It can be observed that all Al(III) complexes show complex spectra with many crests and broad peaks, which is consistent with the adoption of the less symmetric *mer*-configuration. This observation agrees with the NMR results in solution, which indicated that the *mer*-isomer is observed for all the Al(III) complexes measured. The complexes Inq_3 , $\text{In(qCH}_3)_3$ and In(qCl)_3 have better resolved spectra than the Al(III) analogues, presenting less and sharper peaks, a fact that suggests the occurrence of the more symmetric *fac*-isomer. This is also in accordance with the configurational preference for this isomer for all In(III) complexes in solution, as observed by NMR. On the other hand, the ^{13}C CP/MAS NMR spectra of the complexes $\text{In(qNO}_2)_3$ and In(qBr)_3 are very similar to those of the corresponding Al(III) derivatives. When combining this fact with the FTIR results, which indicated nearly superimposed spectra in the $1400\text{--}800\text{ cm}^{-1}$ region for $\text{M(qNO}_2)_3$ and M(qBr)_3 ($\text{M} = \text{Al(III)}$, In(III)), it can be proposed that, for both metals, these substituted complexes adopt the *mer*-configuration in the solid phase.

These results are a strong indication that all Al(III) complexes studied occur as the *mer*-isomer, both in solution and in solid phase. For the In(III) complexes, despite all of them being *fac*-in solution, their configuration in the solid phase depends on the substituent. These results evidence that *mer*- and *fac*-are the most stable molecular configurations of Al(III) and In(III) complexes, respectively. The preference of $\text{In(qNO}_2)_3$ and In(qBr)_3 for the *mer*-isomer in the solid phase can be explained by the

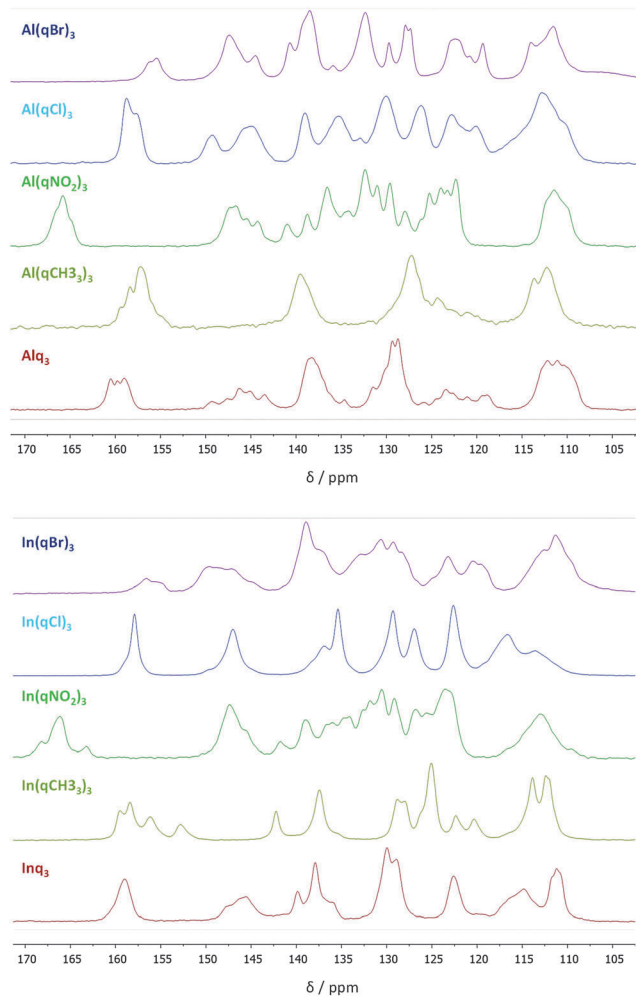


Fig. 6 ^{13}C CP/MAS NMR spectra of the solid Mq_3 complexes, $\text{M} = \text{Al}(\text{III})$ (top), $\text{In}(\text{III})$ (bottom).

effect of these substituents on the intermolecular interactions each isomer can establish. Recently, it was shown that *mer*- Alq_3 and *mer*- Gaq_3 present higher melting temperatures, T_m , and enthalpies of sublimation, $\Delta_{\text{sub}}H_m^0$, than *fac*- Inq_3 , indicating that the *mer*-configuration leads to stronger cohesive forces in the solid phase.^{6d} With the introduction of the highly polarizing 5- NO_2 and the bulky 7-Br substituents the gain in cohesive energy in the *mer*-relative to the *fac*-isomer is probably enhanced, thus overcoming the molecular preference for the *fac*-configuration in these $\text{In}(\text{III})$ complexes. For the unsubstituted Alq_3 and Inq_3 these results agree with the previous literature reports, which indicate that in solid and solution the most stable isomer of Alq_3 is the *mer*- and of Inq_3 is the *fac*-^{5,6,8}

Table 1 presents the computationally calculated *mer* \rightarrow *fac*-electronic isomerization energies, $\Delta_{\text{el}}E_{0\text{K}}(\text{mer} \rightarrow \text{fac})$, for the complexes studied, at the M06-2X/6-31+G(d,p)/SDD level of theory. For the unsubstituted complexes the calculated enthalpies of isomerization, $\Delta H_{298\text{K}}(\text{mer} \rightarrow \text{fac})$ (including ZPE and thermal correction to enthalpy to $T = 298.15$ K), give virtually the same results, confirming that these corrections effectively cancel out in the *mer* \rightarrow *fac*-reaction scheme. Hence, it is a valid approximation

Table 1 Calculated *mer* \rightarrow *fac* isomerization electronic energies in the gas phase, at $T = 0$ K, $\Delta_{\text{el}}E_{0\text{K}}(\text{mer} \rightarrow \text{fac})$, for the Mq_3 complexes studied, obtained at the M06-2X/6-31+G(d,p)/SDD level of theory

Metal	Compound (R)	$\Delta_{\text{el}}E_{0\text{K}}(\text{mer} \rightarrow \text{fac})^a/\text{kJ mol}^{-1}$
Al	Alq_3 (R = H)	20 (19)
	$\text{Al}(\text{qCH}_3)_3$ (R = 2- CH_3)	44
	$\text{Al}(\text{qNO}_2)_3$ (R = 5- NO_2)	21
	$\text{Al}(\text{qCl})_3$ (R = 5-Cl)	20
	$\text{Al}(\text{qBr})_3$ (R = 7-Br)	30
Ga	Gaq_3 (R = H)	16 (13)
In	Inq_3 (R = H)	13 (12)
	$\text{In}(\text{qCH}_3)_3$ (R = 2- CH_3)	30
	$\text{In}(\text{qNO}_2)_3$ (R = 5- NO_2)	14
	$\text{In}(\text{qCl})_3$ (R = 5-Cl)	14
	$\text{In}(\text{qBr})_3$ (R = 7-Br)	23

^a In parenthesis are shown the values of $\Delta H_{298\text{K}}(\text{mer} \rightarrow \text{fac})$ corrected for ZPE and thermal corrections to enthalpy to $T = 298.15$ K.

to evaluate energetics based solely on $\Delta_{\text{el}}E_{0\text{K}}(\text{mer} \rightarrow \text{fac})$. As previously reported, computational methods can predict the lower preference of Inq_3 , relative to Alq_3 and Gaq_3 , for the *mer*-isomer,^{6d,10} but are unable to reproduce the higher stability of the *fac*-isomer for all $\text{In}(\text{III})$ complexes. However, a regular trend in $\Delta_{\text{el}}E_{0\text{K}}(\text{mer} \rightarrow \text{fac})$ with the substituent can be observed for $\text{Al}(\text{III})$ and $\text{In}(\text{III})$ complexes, 2- CH_3 and 7-Br increase the relative stability of the *mer*-isomer and the other substituents have a negligible effect compared to the unsubstituted Mq_3 . This effect is larger for 2- CH_3 than for 7-Br because the substituents in position 2 of 8-hydroxyquinolate are placed in very short contact with the other ligands, whereas in position 7 they are significantly further away (optimized geometries are presented as the ESI^\ddagger).

The observation that bulky groups in interior positions of the complex further increase the relative stability of the *mer*-isomer is in accordance with the fact that steric repulsions between ligands are generally stronger in the *fac*-configuration.¹⁴ This is probably an additional contribution for $\text{In}(\text{qBr})_3$ adopting the *mer*-configuration in the solid phase, as observed experimentally. It is also worth noting that for all substituents $\Delta_{\text{el}}E_{0\text{K}}(\text{mer} \rightarrow \text{fac})$ is always greater for $\text{Al}(\text{III})$. This is consistent with the experimental results in relative terms (higher tendency of $\text{In}(\text{III})$ complexes to be *fac*-), and is probably related with the smaller size of Al. A smaller metal atom leads to shorter M–ligand bonds and accentuates intraligand repulsion, thus increasing the energetic gain associated to the *mer*-configuration. On the other hand, the optimized geometries of the *mer*/*fac*- Mq_3 complexes studied (presented as the ESI^\ddagger), as well as the reported X-ray crystallographic structures of *mer*- Alq_3 , *mer*- Inq_3 and *fac*- Inq_3 ,^{6a,7a,8} evidence a slightly larger variation of the M–ligand bond lengths (M–N and M–O) within the *mer*-isomers. This is related with the existence of three linear N–M–O bond arrangements in the more symmetric *fac*-isomer versus one N–M–N, one O–M–O and one N–M–O in the *mer*-isomer.

Based on the experimental and computational results it is anticipated that the rationale behind *mer*/*fac*-isomerization in Mq_3 compounds resembles the general accepted arguments for

typical *mer/fac*-complexes, like $M(\text{CO})_3(\text{PR}_3)_3$.¹⁴ The facial arrangement is generally electronically favored because it has three linear X–M–Y configurations of atoms/groups/ligands with different donor/acceptor characteristics in the spectrochemical series. On the contrary, the meridional arrangement has only one such configuration, while the two others place equal groups in a X–M–X alignment. The X–M–Y arrangement is usually preferred because it avoids two ligands with identical electronic characteristics competing for the same metal “d” orbital. Hence, in the case of Mq_3 a linear N–M–O arrangement is expected to be electronically preferred over N–M–N or O–M–O. On the other hand, repulsive intraligand steric interactions are reduced in the *mer*-isomer, and this effect is more important for bulkier ligands and smaller metals. The preferred configuration of a given complex results from the compromise between the bonding and steric factors. This is consistent with the preference of Al(III) complexes for the *mer*-isomer – the steric repulsions in the *fac*-isomer are stronger and overcome the energetic advantage of establishing three linear N–M–O bonding configurations. This tendency also holds for the Mq_3 complexes of Fe(III) and Co(III), which have atomic and ionic radii comparable to those of Al and Ga, and were observed as the *mer*-isomers in the crystal phase.¹⁵ The *fac*-isomer is favoured in In(III) complexes because the size of the metal is larger and the bonding factor prevails. To have a quantitative idea of the influence of the metal on the intraligand steric repulsions the electronic interaction energy, $\Delta_e E_{\text{OK}}(\text{int.})$, between the three 8-hydroxyquinolate ligands in Alq_3 and Inq_3 was evaluated at the M06-2X/6-31+G(d,p) level of theory according to the following reaction: $3\text{q}^{\bullet} \rightarrow [\text{q}_3^{\bullet}]$, where q^{\bullet} is the 8-hydroxyquinolate radical and $[\text{q}_3^{\bullet}]$ represents the intermolecular complex formed between the three ligands with the geometry they adopt in the respective Mq_3 complexes (the metal was removed from the Mq_3 optimized geometry and a single point energy calculation, without BSSE correction, was performed in the resulting aggregate; for q^{\bullet} were considered its relaxed optimized geometry and the geometry it adopts in the complex). The results, presented as the ESI,[†] clearly indicate that for Alq_3 the intraligand repulsive interactions are considerably larger than for Inq_3 , considering both the *mer*- and *fac*-isomers. The average calculated M–N and M–O distances are, respectively: 2.07 and 1.88 Å for *mer*- Alq_3 , and 2.25 and 2.07 Å for *mer*- Inq_3 .

Trends in M–ligand bond dissociation energies

The UV-Vis spectra in CH_2Cl_2 for all the complexes studied and the free ligands are presented as the ESI.[†] No noteworthy spectral differences are observed between the Al(III) and In(III) complexes, and hence UV-Vis is unable to distinguish between the *mer*- and *fac*-isomers. When comparing with the corresponding free ligands all complexes show the expected bathochromic and hyperchromic shifts. A small but regular bathochromic shift (≈ 6 nm) in the highest wavelength peak can be noticed for the In(III) complexes relative to the Al(III) analogues. This can indicate a slightly more extensive electronic conjugation in the In(III) complexes and will be discussed in more detail later. Fig. 7 shows the UV-Vis spectra of the Mq_3 , $\text{M}(\text{qCH}_3)_3$ and $\text{M}(\text{qNO}_2)_3$ complexes ($\text{M} = \text{Al(III), In(III)}$), evidencing significant

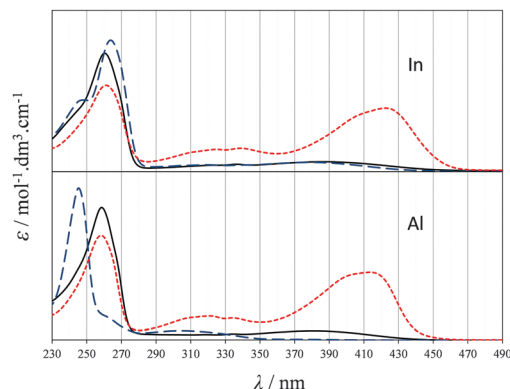


Fig. 7 UV-Vis spectra, in CH_2Cl_2 , of selected $\text{M}(\text{qR})_3$ complexes, $\text{M} = \text{Al(III)}$ (bottom), In(III) (top): $\text{R} = \text{H}$ (black solid lines); 2-CH_3 (blue dashed lines); 5-NO_2 (red dotted lines).

bathochromic and hyperchromic shifts in the compounds with the -NO_2 substituent, and a total and a partial ligand decomplexation in $\text{Al}(\text{qCH}_3)_3$ and $\text{In}(\text{qCH}_3)_3$, respectively. In the cases of the $\text{M}(\text{qNO}_2)_3$ complexes comparison with the UV-Vis spectrum of the corresponding free quinoline ligand (presented as the ESI,[†]) reveals that the main reason for the spectral differences is the presence of the strong chromophore -NO_2 group, and no significant evidences for charge transfer were found. For $\text{In}(\text{qCH}_3)_3$ the existence of the complexation equilibrium was confirmed by observing the spectral changes with varying initial concentrations of the complex. The results are presented as the ESI,[†] and show the expected decrease of the ligand's relative concentration for higher initial concentrations of the complex. The virtually complete decomplexation of $\text{Al}(\text{qCH}_3)_3$ in solution was observed before by ^1H NMR; however, due to the higher sample concentrations generally used in NMR, the partial decomplexation of $\text{In}(\text{qCH}_3)_3$ is only observed if the lower concentrations required by UV-Vis are used (in the ^1H NMR spectrum no free ligand was detected). These observations evidence the weakening effect of the 2-CH_3 substituent on the M–ligand bond.

The calculated HOMO/LUMO energies, using M06-2X/6-31+G(d,p)/SDD (presented as the ESI,[†]), indicate that the effects of metal and substituent on band gap are small (≈ 0.1 eV) in both the *mer*- and *fac*-isomers. Nevertheless, the molecular conformation has a slightly stronger effect, particularly if the metal is Al(III), with the *fac*-isomers presenting a band gap 0.2–0.3 eV higher than the corresponding *mer*-analogues.

The relative M–ligand bond dissociation energies for the complexes studied in the gas phase, expressed as $E_{\text{cm},1/2}$, were evaluated by ESI-MS-MS of the ions $[\text{Mq}_3 + \text{H}]^+$, $[\text{Mq}_3 + \text{Na}]^+$, $[\text{M}(\text{qR})_3 + \text{H}]^+$, $[\text{Mq}_2]^+$ and $[\text{M}(\text{qR})_2]^+$ at variable collision energy (see the ESI,[†] for spectra examples). The main fragmentation reactions observed in all spectra are represented in Fig. 8. Although the two fragmentation reactions are quite different in nature (heterolytic without metal reduction vs. homolytic with metal reduction), the relative trends with the substituents are valid and comparable. The results for the unsubstituted complexes are presented in Table 2. A decrease of $E_{\text{cm},1/2}$ with the

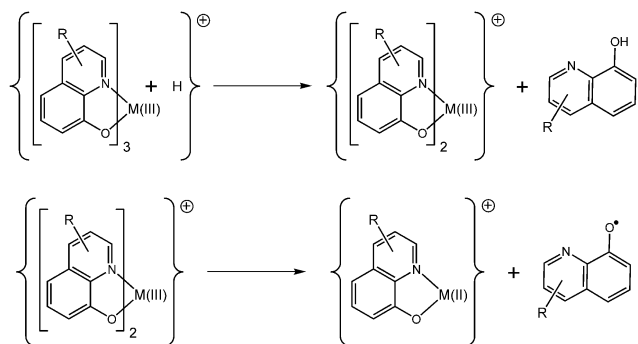


Fig. 8 Fragmentation reactions used to evaluate the relative M–ligand bond dissociation energies in the ion complexes $[Mq_3 + H]^+$ and $[Mq_2]^+$ studied by ESI-MS-MS.

increase of the metal size ($Al < Ga < In$) could in principle be expected because of the lengthening of the M–ligand bonds. However, for both the $[Mq_3 + H]^+$ and $[Mq_3 + Na]^+$ ions a non-monotonous tendency in $E_{cm,1/2}$ ($Al > In > Ga$) with the size of the metal is observed. More specifically, this result supports that Inq_3 adopts a different configuration from Alq_3 and Gaq_3 . According to the results presented before it is safe to assume that, also in the gas phase, Alq_3 and Gaq_3 are *mer*- and Inq_3 is *fac*-. From Alq_3 to Gaq_3 , $E_{cm,1/2}$ decreases due to the longer and weaker M–ligand bonds in the $Ga(III)$ complex. In Inq_3 the lengthening of the M–ligand bonds is partially compensated by the isomerization to the *fac*-isomer, which, as referred before, leads to stronger M–ligand bonding when the steric factor is less significant. The higher $E_{cm,1/2}$ values observed for $[Mq_3 + Na]^+$ suggest the establishment of $Na^+ \cdots O$ and/or $Na^+ \cdots \pi$ interactions with the 8-hydroxyquinolinate ligands, which are also broken in the process.

For the $[Mq_2]^+$ complexes the trend in $E_{cm,1/2}$ is more regular, decreasing monotonously with the increase of the metal size; e.g.: homolytic bond dissociation energies (in kJ mol^{-1}), at $T = 298 \text{ K}$, for $Al-O$ (502 ± 11), $Ga-O$ (374 ± 21) and $In-O$ (346 ± 30).¹⁶ This is in accordance with the tetrahedral geometry adopted by Mq_2 complexes – confirmed by geometry optimization at the $M06-2X/6-31+G(d,p)/SDD$ level (see the ESI†) – which doesn't have X–M–X nor X–M–Y linear bond

Table 2 Relative metal–ligand bond dissociation energies, as evaluated by the values of $E_{cm,1/2}$ obtained by ESI-MS-MS, for the unsubstituted Mq_3 complexes

Ion	Compound	$E_{cm,1/2}^a/\text{eV}$
$[Mq_3 + H]^+$	Alq_3	0.859 ± 0.002
	Gaq_3	0.380 ± 0.004
	Inq_3	0.60 ± 0.03
$[Mq_2]^+$	Alq_3	5.29 ± 0.04
	Gaq_3	3.79 ± 0.04
	Inq_3	1.88 ± 0.05
$[Mq_3 + Na]^+$	Alq_3	2.32 ± 0.02
	Gaq_3	1.73 ± 0.02
	Inq_3	1.98 ± 0.01

^a Errors given as the standard deviation.

arrangements and virtually eliminates intraligand interactions. These results support that the structure and energetics of octahedral Mq_3 complexes are ruled by the intrinsic electronic factors of M–ligand bonding and intraligand interactions. The results for the unsubstituted Mq_3 and Mq_2^+ corroborate the adopted structures and the interplay between the bonding and steric factors in these complexes.

The results of $E_{cm,1/2}$ for the substituted complexes are presented in Table 3. Fig. 9 shows the graphical representation of $E_{cm,1/2}$ for all the Mq_3 complexes studied. It can be observed that substituents have a significant effect on the strength of the M–ligand bond and that approximately the same tendency with the substituent is followed for both metals. The $Al(III)$ show reproductively higher $E_{cm,1/2}$ values than the $In(III)$ complexes, suggesting that the substituents produce similar effects on both complexes. The weakening of the M–ligand bond for $R = 2-CH_3$ is explained by the increased intraligand steric repulsions brought about by the presence of the more bulky methyl groups in a central and interior position of the complex. These results are in agreement with the decomplexation of $Al(qCH_3)_3$ and $In(qCH_3)_3$ in solution, as observed by 1H NMR

Table 3 Relative metal–ligand bond dissociation energies, as evaluated by the values of $E_{cm,1/2}$ obtained by ESI-MS-MS, for the substituted Mq_3 complexes

Ion	R	$E_{cm,1/2}^a/\text{eV}$	
		M = $Al(III)$	M = $In(III)$
$[M(qR)_3 + H]^+$	H	0.859 ± 0.002	0.60 ± 0.03
	2- CH_3	0.72 ± 0.04	0.45 ± 0.04 ^b
	5- NO_2	1.02 ± 0.06	
	5-Cl	0.71 ± 0.06	0.55 ± 0.02
	7-Br	0.89 ± 0.01	0.71 ± 0.04
$[M(qR)_2]^+$	H	5.29 ± 0.04	1.88 ± 0.05
	2- CH_3	—	2.00 ± 0.03
	5- NO_2	—	1.84 ± 0.03
	5-Cl	—	1.61 ± 0.04
	7-Br	—	1.55 ± 0.02

^a Errors given as the standard deviation. ^b In the ESI-MS of this complex, this ion is superimposed to a doubly charged ion, and could not be studied by ESI-MS-MS.

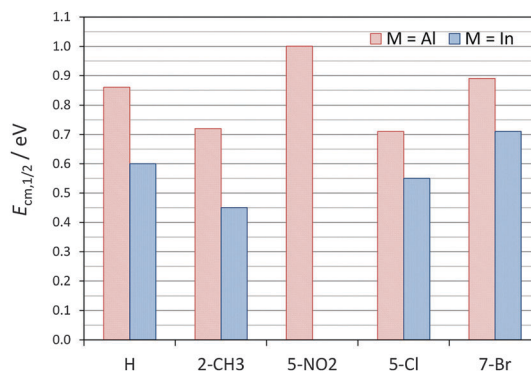


Fig. 9 Graphical representation of $E_{cm,1/2}$ (as measured by ESI-MS-MS) for the Mq_3 complexes studied (M = $Al(III)$, $In(III)$).

and UV-Vis. Solvation effects and the existence of competing complexation equilibria in solution (the relative magnitude of which depend on the identity of the metal) are probably the reason why decomplexation in solution is more extensive in the Al(III) complex, despite its higher value of $E_{\text{cm},1/2}$.

The comparison between the values of $E_{\text{cm},1/2}$ for Al(III) and In(III) complexes suggests that the effect of introducing the 2-CH₃ substituent is more marked in the case of In. This is consistent with the molecular configurations adopted by these complexes, *mer*- for Al(III) and *fac*- for In(III), as evidenced in this work by other techniques. As illustrated in Fig. 10, while in the *mer*-complex one methyl substituent is further away from the other two, the *fac*-isomer places all three methyl groups in close proximity, thus contributing for stronger intraligand repulsions and consequently a more noticeable weakening of the M–ligand bond.

The ESI-MS-MS results suggest stronger M–ligand bonding for the complexes with the 5-NO₂ substituent. In principle, the presence of the strong electron withdrawing –NO₂ group could lead to the weakening of the M–ligand bond by decreasing the negative charge of the coordinating oxygen atom and thus reducing the electrostatic interaction with the M³⁺ ion. As previously observed, the UV-Vis spectra of these compounds show a significant bathochromic and hyperchromic shifts; which, apart from the presence of the strong –NO₂ chromophore, can also have a contribution from a more pronounced electron delocalization throughout the complex. This is supported by the comparison of the ¹H NMR spectra of the free ligands and the respective Al(III) and In(III) complexes – for R = 5-NO₂ there are marked differences in the chemical shifts of some protons between the free ligand and the complex, while for the other substituents the differences upon complexation are less significant. The greater alterations in the chemical environment of the 8-hydroxyquinoline protons upon complexation suggests the existence of some electronic and/or stereochemical factor that is more relevant in the R = 5-NO₂ complexes. The comparison between the 2D ¹H NOESY NMR spectra of Alq₃, Al(qNO₂)₃ and In(qNO₂)₃ suggests that no additional stereochemical effects exist in the M(qNO₂)₃ complexes. On the other hand, a greater electron delocalization in these molecules is consistent with these observations, since it leads to a different charge distribution

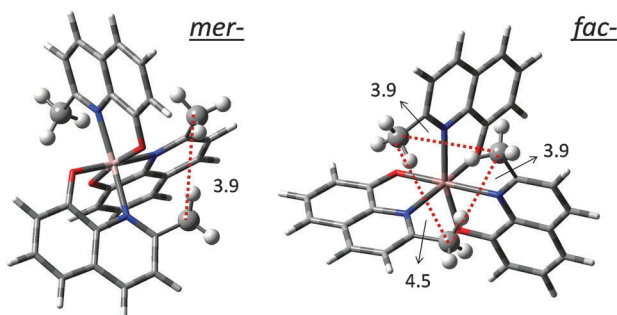


Fig. 10 Optimized geometries, at the M06-2X/6-31+G(d,p)/SDD level of theory, of *mer*-Al(qCH₃)₃ and *fac*-In(qCH₃)₃, evidencing the relative positions of the methyl substituents in the two isomers (distances shown are in Å).

in the ligands and influences the chemical shifts. The other important consequence of the higher degree of conjugation in the 5-NO₂ complexes is the strengthening of the M–ligand bonds, as indicated by the ESI-MS-MS results. Examination of the 2D ¹H NOESY and ¹⁵N HMBC NMR results for Al(qNO₂)₃ indicates the existence of two types of non-equivalent aromatic nitrogens in a 2:1 ratio (see the ESI† for details). One ¹⁵N chemical shift is attributed to the ligand with the N–M–O bonding relation (corresponding to the ligand more to the left in the *mer*-Mq₃ isomer in Fig. 1), and the other ¹⁵N chemical shift is attributed to the two equivalent nitrogens of the other two ligands with N–M–N relations. In fact, the N–M–O ligand is the one for which the ¹H chemical shifts are more deshielded and more similar to the *fac*-In(qNO₂)₃ complex, in which all ligands have the same N–M–O bond configuration. It is interesting to note that, although –Cl and –Br are substituents with similar electronic properties, they have opposite effects on $E_{\text{cm},1/2}$. Stereochemical effects can be neglected in both cases – in position 7 of 8-hydroxyquinolate the bulky –Br group is relatively far from the other ligands in the complex and no significant intramolecular steric repulsions are expected (if these were important they would probably decrease $E_{\text{cm},1/2}$ relative to the unsubstituted Mq₃, which is not the case). Since the distinct effects of the halogen substituents, 5-Cl and 7-Br, cannot be adequately rationalized by stereochemical and/or electrostatic considerations alone, these results support that the M–ligand bond has a significant covalent character.

The calculated heterolytic M–ligand bond dissociation energies, at $T = 0$ K, $\Delta_{\text{el}}E_{0\text{K}}(\text{BD})$ for the complexes studied are presented in Table 4. The calculated energies correspond to the reaction: $\text{M}(\text{qR})_3 \rightarrow \text{M}(\text{qR})_2^+ + \text{q}(\text{R})^-$, considering the two *mer*- and *fac*-isomers. The influence of the ZPE and thermal corrections to enthalpy to $T = 298.15$ K on the bond dissociation energies was found to be only meaningful in absolute terms but to yield the same results in comparative terms. Hence, these corrections can be neglected for the relative evaluation of bonding energetics. To assure that the reaction $\text{M}(\text{qR})_3 \rightarrow \text{M}(\text{qR})_2^+ + \text{q}(\text{R})^-$ is a valid approximation to the fragmentation process studied experimentally (Fig. 8), the values of $\Delta_{\text{el}}E_{0\text{K}}(\text{BD})$ were also calculated for the reaction: $[\text{M}(\text{qR})_3 + \text{H}]^+ \rightarrow [\text{M}(\text{qR})_2]^+ + \text{Hq}(\text{R})$, for M = Al (results presented as the ESI†) – the same tendency with the substituent was verified. This is reasonable because M(qR)₃ and q(R)[–] have comparable relative affinities for H⁺, and this contribution can be neglected if comparing substitution trends.

As it was also the case in the evaluation of *mer*-/*fac*-isomerism, the DFT computational results agree only partially with experiment. The computational results correctly predict the lower bond dissociation energy for both isomers of the R = 2-CH₃ complexes. The relative trends in bond energetics for the halogenated complexes are also adequately reproduced by the DFT results. The reason why the M–ligand bond is stronger in M(qBr)₃ (R = 7-Br) can be related with the destabilization of the $[\text{M}(\text{qBr})_2]^+$ product, as evidenced by its significantly lower value of $E_{\text{cm},1/2}$ (Table 3). However, the results for R = 5-NO₂ are in contradiction with experiment, with the computational DFT results following the expected behavior if the M–ligand bond

Table 4 Calculated heterolytic bond dissociation energies, at $T = 0$ K, $\Delta_{\text{el}}E_{0\text{K}}(\text{BD})$, for the Mq_3 complexes studied, obtained at the M06-2X/6-31+G(d,p)/SDD level of theory

Metal	R	$\Delta_{\text{el}}E_{0\text{K}}(\text{BD})^a/\text{kJ mol}^{-1}$	
		<i>mer</i> -	<i>fac</i> -
Al	H	667 (656)	647 (637)
	2-CH ₃	623	579
	5-NO ₂	660 (649)	640
	5-Cl	662	641
	7-Br	680	650
Ga	H	627	610
In	H	671 (661)	658 (648)
	2-CH ₃	643	612
	5-NO ₂	658	644 (635)
	5-Cl	663	650
	7-Br	681	658

^a In parenthesis are shown the values of $\Delta H_{298\text{K}}(\text{BD})$ corrected for ZPE and thermal corrections to enthalpy to $T = 298.15$ K.

was assumed to be ruled by electrostatic interactions, as it was previously suggested in the literature.^{11b} If considering that the Al(III) complexes are *mer*- and the In(III) are *fac*-, the computational results also correctly predict stronger M–ligand bonding for the Al(qR)₃ complexes for all substituents.

The trend in M–ligand bond strength for the tetra-coordinated M(qR)₂ complexes (Table 3) is clearly different from that observed for the octahedral M(qR)₃ compounds. The structure of all M(qR)₂ species was confirmed to be tetrahedral by M06-2X/6-31+G(d,p)/SDD optimization calculations (presented as the ESI†). In this geometry the two 2-CH₃ substituents are sufficiently far away from each other to practically eliminate steric repulsions. The increase in $E_{\text{cm},1/2}$ for M(qCH₃)₂⁺ relative to Mq_2^+ (R = H) can be explained by the inductive effect of the methyl group, which increases the negative charge on the coordinating O and N atoms and consequently the electrostatic interactions with the central metal. The effect of the halogens 5-Cl and 7-Br can be understood by their electron withdrawing capabilities by inductive effect, which decreases the negative charge on the coordinating O and N atoms (the more pronounced decrease of $E_{\text{cm},1/2}$ for 7-Br is due to its closer proximity). The same reasoning can be applied to the 5-NO₂ substituent, a strong electron withdrawer by inductive and mesomeric effects. The NBO partial charges for all the 8-hydroxyquinolate ligands were calculated at the M06-2X/6-31+G(d,p) level and the values of the negative charges on the coordinating N and O atoms compare well with the experimental results for $E_{\text{cm},1/2}$ (detailed results presented as the ESI†). Tetrahedral M(qR)₂ complexes have less participation of the metal “d” orbitals in bonding (sp^3 hybridization) and the absence of linear X–M–X or X–M–Y bond arrangements prevents an effective through-ligand orbital overlap (mediated by the metal “d” orbitals). Hence, there is less electronic conjugation between the ligands and this can explain the fact of –NO₂ not having the same effect of strengthen the M–ligand bond as in the case of In(qNO₂)₃. These results indicate that M–ligand bonding in Mq_2 tetrahedral complexes is more electrostatic in nature than in the octahedral Mq_3 , for which

electrostatic considerations do not suffice to explain the experimental observations.

Bonding in Mq_3 complexes

This study gives insights on the nature of the chemical bond in Mq_3 octahedral complexes. The global results indicate that in these complexes the M–ligand bond has strong covalent character and cannot be rationalized solely on electrostatic terms. This is in agreement with a recent literature report, wherein the authors admit the existence of electron delocalization between the metal and the ligand in the complex of Crq₃.^{11a} This allows for the existence of significant through-ligand conjugation, which is more notorious in the cases of the M(qNO₂)₃ complexes. This picture is consistent with the trends in the $E_{\text{cm},1/2}$ values and the observed NMR and UV-Vis spectral features. Since the octahedral metal center can adopt a sp^3d^2 hybridization scheme, this electronic conjugation is probably mediated by the metal “d” orbitals. The bonding advantage of the *fac*-isomer can also be rationalized on these grounds. As schematically shown in Fig. 11, in the N–M–N and O–M–O bonding configurations of the *mer*-isomer the orbitals of the two coordinating N or O atoms are nearly orthogonal, thus reducing substantially the degree of through-ligand conjugation. On the other hand, the more parallel orbitals of the coordinating N and O atoms in N–M–O bonding (three in *fac*- and one in *mer*-) enable an extensive overlap with the metal “d” orbital of adequate geometry. The more extensive electron delocalization contributes for stronger M–ligand bonding in Mq_3 complexes. The preference of Tlq₃ for the *mer*-isomer⁹ can also be understood by this reasoning. The much larger size of Tl relative to O and N leads to a poorer orbital overlap, and a weaker through-ligand conjugation. Hence, the bonding advantage in the *fac*-isomer is reduced and the steric factor, which favours the *mer*-isomer, prevails. It is important to note that this rationale deviates a bit from that discussed in the previous section for typical *mer*-/*fac*-isomers, like the M(CO)₃(PR₃)₃ compounds.¹⁴ In the particular case of Mq_3 complexes the main bonding advantage in X–M–Y linear arrangements comes from the fact that the orbitals of the ligands (π in the N and sp^3 in the O) are nearly parallel to each other and both interact with the same metal “d” orbital, enabling direct through-ligand conjugation. On the other hand, in X–M–X relations the orbitals of the two ligands are perpendicular and each of them overlaps preferentially with a different metal “d” orbital, thus reducing electron delocalization. In the X–M–X arrangements there is virtually no competition between equal atoms for the same metal “d” orbital. In the X–M–Y relations the atoms interacting

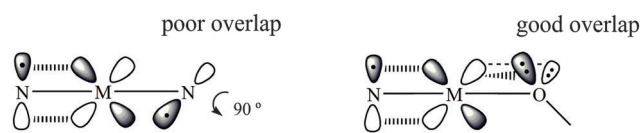


Fig. 11 Schematic representation of the through-ligand orbital overlap respecting the N–M–N (left) and N–M–O (right) bonding relations in Mq_3 complexes.

Table 5 Relative dissociation energies, as evaluated by the values of $E_{\text{cm},1/2}$ obtained by ESI-MS-MS, for some relevant Mq_3 supramolecular aggregates

Ion	Compound	$E_{\text{cm},1/2}/\text{eV}$
Dimers with Na^+ : $[(\text{Mq}_3)_2 + \text{Na}]^+ \rightarrow \text{Mq}_3 + [\text{Mq}_3 + \text{Na}]^+$ $[(\text{Mq}_3)_2 + \text{Na}]^+$	Alq_3	0.69 ± 0.02
	GaQ_3	0.64 ± 0.01
	Inq_3	0.59 ± 0.01
Mq_3 - Mq_2 complexes: $[(\text{Mq}_3)-(\text{Mq}_2)]^+ \rightarrow \text{Mq}_3 + \text{Mq}_2^+$ $[(\text{Mq}_3)-(\text{Mq}_2)]^+$	Alq_3	1.48 ± 0.01
	GaQ_3	1.05 ± 0.01
	Inq_3	1.46 ± 0.01

with the same metal “d” orbital have opposite electronic characteristics – the coordinating N and O integrate, respectively, relatively strong π -acceptor and π -donor moieties – and this probably also contributes for a stronger M–ligand bond.

The analysis of the computational results indicates that the theoretical methods generally used for studying these systems (mostly DFT and MP2)^{6d,10} are inadequate. This is possibly due to a bad description of the M–ligand bond or of electron correlation in Mq_3 complexes by these methods.

Exploring the supramolecular chemistry of Mq_3 complexes

The formation of some supramolecular complexes involving the Mq_3 complexes was also detected in the mass spectrometry study. This was further investigated by ESI-MS-MS for the unsubstituted Alq_3 , GaQ_3 and Inq_3 complexes. The main species observed were $[(\text{Mq}_3)_2 + \text{Na}]^+$ and $[(\text{Mq}_3)-(\text{Mq}_2)]^+$ aggregates. The experimental values of $E_{\text{cm},1/2}$ for these supramolecular aggregates are presented in Table 5.

Based on the composition and fragmentation of the $[(\text{Mq}_3)_2 + \text{Na}]^+$ aggregates, and the monotonous decrease of $E_{\text{cm},1/2}$ with the increase of the metal size, a supramolecular structure where Na^+ is sandwiched between two Mq_3 molecules through cation $\cdots \text{O}$ and/or cation $\cdots \pi$ interactions can be suggested. The tendency of Mq_3 complexes to bind Na^+ is also corroborated by the formation of $[\text{Mq}_3 + \text{Na}]^+$ aggregates, as discussed before (see Table 2). The ability of aromatic systems to bind small cations is already well documented in the literature.¹⁷ Concerning the $[(\text{Mq}_3)-(\text{Mq}_2)]^+$ aggregates the variation of $E_{\text{cm},1/2}$ with the metal suggests that intermolecular binding is favoured for *fac*-isomers. The formation of a covalent supramolecular complex, with the two metals bridged by a quinolate ligand, $[\text{q}_2\text{M}-\text{q}-\text{Mq}_2]^+$, can in principle be ruled out because the size and shape of 8-hydroxyquinolate do not allow for a bridged complex without significant steric repulsions. One can also anticipate that aromatic interactions between the ligands are possibly the main driving force for the formation of these aggregates. Although, with the available data, no reliable structures can be proposed, the results demonstrate the ability of Mq_3 complexes to interact with small cations and to form small supramolecular aggregates. This can be helpful for understanding phenomena involving clustering of Mq_3 molecules (e.g. in the deposition of thin-films), and interactions in solution and at surfaces.

Conclusions

In this work the effects of the metal and ligand substitution on the molecular isomerism and M–ligand bond strength in Mq_3 complexes were evaluated by experimental and computational methods. The results show that *mer*-/*fac*-isomerism is ruled by the identity of the metal and is nearly independent of the substituent. The *mer*-isomer is preferred for smaller metals, like Al; the main driving force being the reduction of intraligand steric repulsions relative to the sterically more crowded *fac*-isomer. For bigger metals, like In, the stereochemical repulsions are diluted and the *fac*-isomer is preferred due to stronger M–ligand bonding. The results obtained are fully understandable if assuming that M–ligand bonding has strong covalent character and is not ruled by electrostatics. The covalent bonds involve the ligands (π and non-bonding sp^3) and the metal “d” orbitals, thus allowing for through-ligand electron delocalization. Stronger M–ligand bonding in the *fac*-isomer is explained by the more efficient through-ligand orbital overlap in N–M–O linear bond relations, relative to the N–M–N and O–M–O predominant in the *mer*-isomer. This work also highlights the inadequacy of most computational methods to describe molecular energetics of Mq_3 complexes. The ability of Mq_3 complexes to bind Na^+ and form small supramolecular aggregates in the gas phase was also demonstrated. These new insights on the molecular isomerism and bonding in Mq_3 complexes establish a powerful fundamental basis for understanding their semiconducting properties and provide a guide for the future development of improved organic electronic materials.

Acknowledgements

We thank Fundação para a Ciência e Tecnologia (FCT), Lisbon, Portugal, and the European Social Fund (ESF) for financial support to CIQ, REQUIMTE and LEPABE, University of Porto (Projects: PEst-C/UI/UI0081/2011, FCUP-CIQ-UP-NORTE-07-0124-FEDER-000065, PTDC/AAC-AMB/121161/2010, UID/QUI/50006/2013, UID/EQU/00511/2013-LEPABE), and to the Organic Chemistry Research Unit, University of Aveiro (Project: FCT UID/QUI/00062/2013). C. F. R. A. C. L. also thanks FCT and the European Social Fund (ESF) under the third Community Support Framework (CSF) for the award of the Research Grant SFRH/BPD/77972/2011.

Notes and references

- (a) A. Curioni and W. Andreoni, *J. Am. Chem. Soc.*, 1999, **121**, 8216; (b) B. C. Lin, C. P. Cheng, Z.-Q. You and C.-P. Hsu, *J. Am. Chem. Soc.*, 2005, **127**, 66; (c) C. Pérez-Bolívar, S. Takizawa, G. Nishimura, V. A. Montes and P. Anzenbacher, *Chem. – Eur. J.*, 2011, **17**, 9076; (d) Y. Shirota and H. Kageyama, *Chem. Rev.*, 2007, **107**, 953; (e) C. H. Chen and J. Shi, *Coord. Chem. Rev.*, 1998, **171**, 161; (f) S. A. Van Slyke, C. H. Chen and C. W. Tang, *Appl. Phys. Lett.*, 1996, **69**, 2160; (g) S. Scholz, B. Lüssem and K. Leo, *Appl. Phys. Lett.*, 2009, **95**, 183309; (h) J. C. S. Costa, R. J. S. Taveira, C. F. R. A. C. Lima, A. Mendes and L. M. N. B. F. Santos, *Opt. Mater.*, 2016, **58**, 51.

- 2 C. W. Tang and S. A. Van Slyke, *Appl. Phys. Lett.*, 1987, **51**, 913.
- 3 (a) D. Z. Garbuzov, V. Bulovic, P. E. Burrows and S. R. Forrest, *Chem. Phys. Lett.*, 1996, **249**, 433; (b) M. A. Baldo, D. F. Ó'Brien, M. E. Thompson and S. R. Forrest, *Phys. Rev. B: Condens. Matter Mater. Phys.*, 1999, **60**, 14422; (c) S. Paydavosi, K. E. Aidala, P. R. Brown, P. Hashemi, G. J. Supran, T. P. Osedach, J. L. Hoyt and V. Bulovic, *Nano Lett.*, 2012, **12**, 1260; (d) V. V. N. R. Kishore, K. L. Narasimhana and N. Periasamy, *Phys. Chem. Chem. Phys.*, 2003, **5**, 1386; (e) B.-C. Lin, C.-P. Cheng, Z.-Q. Youac and C.-P. Hsu, *Phys. Chem. Chem. Phys.*, 2011, **13**, 20704.
- 4 (a) Y.-W. Yu, C.-P. Cho and T.-P. Perng, *Nanoscale Res. Lett.*, 2009, **4**, 820; (b) I. Hernández and W. P. Gillin, *J. Phys. Chem. B*, 2009, **113**, 14079; (c) M. Brinkmann, B. Fite, S. Pratontep and C. Chaumont, *Chem. Mater.*, 2004, **16**, 4627; (d) V. A. Montes, R. Pohl, J. Shinar and P. Anzenbacher, Jr., *Chem. – Eur. J.*, 2006, **12**, 4523; (e) R. Kumar, P. Bhargava, R. Srivastava and P. Tyagi, *J. Semicond.*, 2015, **36**, 064001; (f) M. L. Ramos, L. L. G. Justino, A. Branco, C. M. G. Duarte, P. E. Abreu, S. M. Fonseca and H. D. Burrows, *Dalton Trans.*, 2011, **40**, 11732; (g) M. L. Ramos, L. L. G. Justino, A. I. N. Salvador, A. R. E. de Sousa, P. E. Abreu, S. M. Fonseca and H. D. Burrows, *Dalton Trans.*, 2012, **41**, 12478; (h) M. L. Ramos, A. R. E. de Sousa, L. L. G. Justino, S. M. Fonseca, C. F. G. C. Geraldés and H. D. Burrows, *Dalton Trans.*, 2013, **42**, 3682.
- 5 (a) M. Muccini, M. A. Loi, K. Kenevey, R. Zamboni, N. Masciocchi and A. Sironi, *Adv. Mater.*, 2004, **16**, 861; (b) C.-K. Tai, Y.-M. Chou and B.-C. Wang, *J. Lumin.*, 2011, **131**, 169; (c) H. Kaji, Y. Kusaka, G. Onoyama and F. Horii, *J. Am. Chem. Soc.*, 2006, **128**, 4292; (d) M. Rajeswaran, T. N. Blanton, C. W. Tang, W. C. Lenhart, S. C. Switalski, D. J. Giesen, B. J. Antalek, T. D. Pawlik, D. Y. Kondakov and N. Zumbulyadis, *et al.*, *Polyhedron*, 2009, **28**, 835; (e) T. Fukushima and H. Kaji, *Org. Electron.*, 2012, **13**, 2985.
- 6 (a) M. Rajeswaran and V. V. Jarikov, *Acta Crystallogr., Sect. E: Struct. Rep. Online.*, 2004, **60**, m217; (b) M. Cölle and W. Brütting, *Phys. Status Solidi*, 2004, **201**, 1095; (c) M. H. Wang, Y. Sawada, K. Saito, S. Horie, T. Uchida, M. Ohtsuka, S. Seki, S. Kobayashi, T. Arai and A. Kishi, *et al.*, *J. Therm. Anal. Calorim.*, 2007, **89**, 363; (d) J. C. S. Costa, C. F. R. A. C. Lima and L. M. N. B. F. Santos, *J. Phys. Chem. C*, 2014, **118**, 21762.
- 7 (a) M. Brinkmann, G. Gadret, M. Muccini, C. Taliani, N. Masciocchi and A. Sironi, *J. Am. Chem. Soc.*, 2000, **122**, 5147; (b) M. Cölle, R. E. Dinnebier and W. Brütting, *Chem. Commun.*, 2002, 2908; (c) M. Cölle, J. Gmeiner, W. Milius, H. Hillebrecht and W. Brütting, *Adv. Mater.*, 2003, **13**, 108; (d) F. Suzuki, T. Fukushima, M. Fukuchi and H. Kaji, *J. Phys. Chem. C*, 2013, **117**, 18809; (e) R. Katakura and Y. Koide, *Inorg. Chem.*, 2006, **45**, 5730.
- 8 M. Rajeswaran and V. V. Jarikov, *Acta Crystallogr., Sect. E: Struct. Rep. Online*, 2003, **59**, m306.
- 9 L. Pecha, J. Bankovskis, A. Kemme, V. Bésy, E. Silin and J. Asaks, *Chem. Heterocycl. Compd.*, 2002, **38**, 695.
- 10 (a) L. S. Sapochak, A. Ranasinghe, H. Kohlmann, K. F. Ferris and P. E. Burrows, *Chem. Mater.*, 2004, **16**, 401; (b) M. Utz, C. Chen, M. Morton and F. Papadimitrakopoulos, *J. Am. Chem. Soc.*, 2003, **125**, 1371.
- 11 (a) A. R. Freitas, M. Silva, M. L. Ramos, L. L. G. Justino, S. M. Fonseca, M. M. Barsan, C. M. A. Brett, M. R. Silva and H. D. Burrows, *Dalton Trans.*, 2015, **44**, 11491; (b) J. Zhang and G. Frenking, *J. Phys. Chem. A*, 2004, **108**, 10296; (c) A. Curioni, M. Boero and W. Andreoni, *Chem. Phys. Lett.*, 1998, **294**, 263; (d) A. Curioni, W. Andreoni, R. Treusch, R. F. Himpsel, E. Haskal, P. Seidler, S. Kakar, T. van Buuren and L. J. Terminello, *Appl. Phys. Lett.*, 1998, **72**, 1575; (e) M. D. Halls and H. B. Schlegel, *Chem. Mater.*, 2001, **13**, 2632; (f) M. Amati and F. Lelj, *Chem. Phys. Lett.*, 2002, **363**, 451; (g) R. L. Martin, J. D. Kress, I. H. Campbell and D. L. Smith, *Phys. Rev. B: Condens. Matter Mater. Phys.*, 2000, **61**, 15804.
- 12 M. J. Frisch, G. W. Trucks, H. B. Schlegel, G. E. Scuseria, M. A. Robb, J. R. Cheeseman, G. Scalmani, V. Barone, B. Mennucci, G. A. Petersson, H. Nakatsuji, M. Caricato, X. Li, H. P. Hratchian, A. F. Izmaylov, J. Bloino, G. Zheng, J. L. Sonnenberg, M. Hada, M. Ehara, K. Toyota, R. Fukuda, J. Hasegawa, M. Ishida, T. Nakajima, Y. Honda, O. Kitao, H. Nakai, T. Vreven, J. A. Montgomery, Jr., J. E. Peralta, F. Ogliaro, M. Bearpark, J. J. Heyd, E. Brothers, K. N. Kudin, V. N. Staroverov, R. Kobayashi, J. Normand, K. Raghavachari, A. Rendell, J. C. Burant, S. S. Iyengar, J. Tomasi, M. Cossi, N. Rega, J. M. Millam, M. Klene, J. E. Knox, J. B. Cross, V. Bakken, C. Adamo, J. Jaramillo, R. Gomperts, R. E. Stratmann, O. Yazyev, A. J. Austin, R. Cammi, C. Pomelli, J. W. Ochterski, R. L. Martin, K. Morokuma, V. G. Zakrzewski, G. A. Voth, P. Salvador, J. J. Dannenberg, S. Dapprich, A. D. Daniels, Ö. Farkas, J. B. Foresman, J. V. Ortiz, J. Cioslowski and D. J. Fox, *Gaussian 09, Revision A.1*, Gaussian Inc, Wallingford, CT, 2009.
- 13 (a) Y. Zhao and D. G. Truhlar, *Theor. Chem. Acc.*, 2008, **120**, 215; (b) L. E. Roy, P. J. Hay and R. L. Martin, *J. Chem. Theory Comput.*, 2008, **4**, 1029.
- 14 A. Holladay, M. R. Churchill, A. Wong and J. D. Atwood, *Inorg. Chem.*, 1980, **19**, 2195.
- 15 (a) L. Pech, Y. A. Bankovsky, A. Kemme and J. Lejejs, *Acta Crystallogr., Sect. C: Cryst. Struct. Commun.*, 1997, **53**, 1043; (b) S. S. S. Raj, I. A. Razak, H.-K. Fun, P.-S. Zhao, F. Jian, X. Yang, L. Lu and X. Wang, *Acta Crystallogr., Sect. C: Cryst. Struct. Commun.*, 2000, **56**, e130.
- 16 Y. R. Luo, *Comprehensive Handbook of Chemical Bond Energies*, CRC Press, Boca Raton, FL2007.
- 17 (a) C. F. R. A. C. Lima, A. M. Fernandes, A. Melo, L. M. Gonçalves, A. M. S. Silva and L. M. N. B. F. Santos, *Phys. Chem. Chem. Phys.*, 2015, **17**, 23917; (b) J. C. Ma and D. A. Dougherty, *Chem. Rev.*, 1997, **97**, 1303; (c) D. A. Dougherty, *Acc. Chem. Res.*, 2013, **46**, 885; (d) A. S. Mahadevi and G. N. Sastry, *Chem. Rev.*, 2013, **113**, 2100; (e) M. J. Webb and N. Bampos, *Chem. Sci.*, 2012, **3**, 2351; (f) S. B. Nimse and T. Kim, *Chem. Soc. Rev.*, 2013, **42**, 366.